

Improved Error Performance in NOMA-based Diamond Relaying

Ferdi KARA, Hakan KAYA

Wireless Communication Technologies Laboratory (WCTLab)

Department of Electrical and Electronics Engineering

Zonguldak Bulent Ecevit University

Zonguldak, TURKEY 67100

Email: {f.kara,hakan.kaya}@beun.edu.tr

Abstract—Non-orthogonal multiple access (NOMA)-based cooperative relaying system (CRS) has emerged as a solution to the spectral inefficiency problem of the conventional CRS thanks to the NOMA integration. Thus, as a subset of the NOMA-CRS, the NOMA-based diamond relaying network (NOMA-DRN) also provides a performance gain in terms of throughput. However, the NOMA-DRN has a poor error performance due to the second phase (uplink), indeed, it has an error floor regardless of the transmit power, power allocation and channel qualities. To address this problem, in this paper, we propose a novel NOMA-DRN scheme where a joint maximum likelihood (JML) decoding is implemented at the destination. Then, we define the performance metrics (i.e., bit error rate (BER) and the diversity order) of the NOMA-DRN with the JML and analyze the computational complexity. Moreover, we demonstrate that the new NOMA-DRN with JML can cope with the error floor penalty of the conventional NOMA-DRN. Hence, a spectral efficient NOMA-CRS scheme can be achieved with high data reliability. Specifically, this improvement can reach to $\sim 20 - 30dB$ in the transmit power which is superb gain in terms of energy efficiency perspective. Furthermore, with the proposed NOMA-DRN with the JML, the full diversity order can be achieved in the low-medium SNR region.

Index Terms—NOMA, diamond relaying, error performance, diversity, joint maximum likelihood detector

I. INTRODUCTION

Cooperative relaying scheme has been one of the most attractive topics since its first applications [1]. It provides a spatial diversity when multiple antennas can not be placed due to the physical limitations at the transmitter and/or receiver. Besides, it also makes possible the higher coverage area when the direct link is not available between the source and the destination. Therefore, the cooperative relaying scheme has been indispensable in the wireless communication evolution as well as the standards for almost two decades. However, the cooperative relaying scheme suffers from the spectral inefficiency since it occupies more than one resource block (time slots) for the forwarding strategies. To address this problem, Non-orthogonal multiple access-based cooperative relaying system (NOMA-CRS) has been proposed in the literature [2] where two consecutive symbols are conveyed simultaneously thanks to the NOMA technique. In NOMA, multiple symbols are merged with different power allocation (PA) coefficients and transmitted to the destination (users) on the same resource block (time, frequency, code). The

interference mitigation is achieved by the successive interference canceler (SIC) at the receivers so that all symbols can be detected [3]. In the first NOMA-CRS paper [2], it is proved that the spectral efficiency is improved compared to the conventional CRS. Then, the NOMA-CRS schemes have attracted a remarkable attention from the both academia and industry where NOMA-CRS schemes have been analyzed in terms of different key performance indicators such as sum-rate, outage probability, energy efficiency, bit error probability over various wireless channel models [4]–[8]. In those works, the theoretical analysis is conducted to reveal the superiority of the NOMA-CRS in terms of capacity and outage probability. However, they mostly assume the perfect SIC and when this assumption is relaxed, the error performance penalty of the NOMA-CRS is presented [9]. In addition to NOMA-CRS with a single relay, multiple relay scenarios have been also considered in the literature [10]. In the multiple relay NOMA-CRS, relay selection schemes have been analyzed in terms of capacity and outage probability.

Moreover, when two relays are located between the source and the destination, as a subset of NOMA-CRS, called NOMA-based diamond relaying network (DRN) is proposed in [11] and the sum-rate expression is derived. Then, the optimum power allocation is studied in [12] to maximize the sum-rate of the NOMA-DRN. However, when the error probability of the NOMA-DRN is analyzed, it is seen that the NOMA-DRN has a poor error performance [13]. Although its performance improvement in terms of sum-rate capacity, the NOMA-DRN has an error floor since it includes an uplink phase of NOMA [14]. Regardless of the transmit power and the PA, the NOMA-DRN fails due to the SIC at the destination. Nevertheless, the authors in [15] prove that the error performance of the uplink NOMA can be improved by using joint maximum-likelihood (JML) detector rather than the SIC detector.

In this paper, to this end, we propose a novel NOMA-DRN with the JML to improve the error performance of the NOMA-DRN with SIC receiver. We revealed that the proposed NOMA-DRN with the JML achieves a good error performance and the error floor exists no more. Therefore, the capacity enhancement of the NOMA-DRN can be provided without the error floor penalty so that a reliable communication is

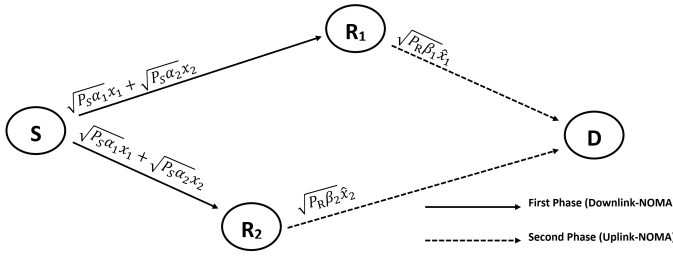


Fig. 1. The illustration of the NOMA-based diamond relaying network

achieved. Moreover, for the same error performance target, the proposed NOMA-DRN with JML can save $\sim 20 - 30dB$ in transmit power which is very promising for the energy-constraint networks such as Internet of Things (IoT) applications. In addition to these advantages, the NOMA-DRN with the JML offers a full diversity order in the low-medium SNR region with a negligible receiver complexity at the destination.

The rest of this paper is organized as follows. The Section II introduces the proposed NOMA-DRN with the JML. The receivers structures and the benchmark scheme have been also given in this section. Then, in Section III, we define the error performance metrics of the NOMA-DRN with the JML such as bit error rate (BER) and diversity order. We also analyze receiver complexity in this section. Moreover, Section IV present computer simulations to evaluate the error performance of the proposed the NOMA-DRN with the JML along with the comparisons of the benchmark. Finally, Section V presents the conclusion remarks.

II. SYSTEM MODEL

In this paper, a device-to-device communication is considered where the source (S) wants to transmit symbols to the destination (D). Due to the large scale objects and/or path-loss, the direct link between $S-D$ is not available, hence a cooperative relaying system is implemented with the help of two decode-forward relays (i.e., R_1 and R_2) which are located between the source and the destination. R_1 is to be closer to the destination whereas R_2 is closer to the source, thus it is called as diamond relaying. The system model is given in the Fig. 1. All nodes are assumed to have a single antenna. Since a cooperative communication is needed and the relays operate in half-duplex mode, the end-to-end (e2e) communication is completed in two phases (time slot) where the first phase is between $S-R_i$ (i.e., $i = 1, 2$) and the second phase is between R_i-D .

In order to alleviate the inefficiency of the conventional CRS, NOMA is implemented at the source for two consecutive symbols of the destination. Hence, the two consecutive symbols are superposition coded with the different PA coefficients and broadcasted to the relays in the first phase (downlink-NOMA). The transmitted total symbol is given by

$$x_{sc} = \sqrt{\alpha_1}x_1 + \sqrt{\alpha_2}x_2 \quad (1)$$

where $\alpha_i, i = 1, 2$ denotes the PA coefficient for the baseband symbol of the x_i where $\alpha_1 > \alpha_2$ is assumed and $\alpha_1 + \alpha_2 = 1$ is satisfied. Hence, the received signal at the relays is

$$y_{R_i} = \sqrt{P_s}(\sqrt{\alpha_1}x_1 + \sqrt{\alpha_2}x_2)h_{SR_i} + n_{R_i}, \quad i = 1, 2 \quad (2)$$

Where P_s is the transmit power of the source. h_{SR_i} is the channel fading coefficient between $S-R_i$ and the envelopes of it follows Nakagami- m distribution with the m_{SR_i} spread and Ω_{SR_i} shape parameters. n_{R_i} is the additive Gaussian noise at the receiver R_i and follows $CN(0, N_0)$.

In the second phase, the relays transmit recovered/detected forms of the related symbols to the destination simultaneously. Thus, the second phase can be called as an uplink NOMA. The received signal at the destination is given by

$$y_D = \sqrt{P_{R_1}}\hat{x}_1h_{R_1D} + \sqrt{P_{R_2}}\hat{x}_2h_{R_2D} + n_D \quad (3)$$

where P_{R_i} is the transmit power of the relay R_i ¹. \hat{x}_1 and \hat{x}_2 are the recovered/detected symbols of the x_1 and x_2 at the relays R_1 and R_2 , respectively. n_D is the additive Gaussian noise at the destination and follows $CN(0, N_0)$.

A. Proposed Receiver Structures

1) *Decoding at the relays:* According to (3), the R_1 forwards x_1 symbols and R_2 transmits x_2 symbols. As seen in (1), the x_1 symbols has higher PA, hence the x_1 symbols can be directly detected at the R_1 by pretending x_2 symbols as noise. To this end, the maximum likelihood (ML) detector at the R_1 is given as

$$\hat{x}_1 = \underset{k}{\operatorname{argmin}} \left| y_{R_1} - \sqrt{P_s\alpha_1}h_{SR_1}x_{1,k} \right|^2, \quad k = 1, 2, \dots, M_1, \quad (4)$$

where $x_{1,k}$ shows the k th point in the M_1 -ary constellation.

On the other hand, since it has lower PA, x_2 can not be directly decoded at R_2 unlike x_1 symbols. An interference mitigation is needed. Thus, we implement an SIC² where x_1 symbols are firstly detected and subtracted from the received signal and then x_2 symbols are detected. The detection steps at the R_2 are given as

$$\hat{x}_2 = \underset{j}{\operatorname{argmin}} \left| y_{R_2}^{(*)} - \sqrt{P_s\alpha_2}h_{SR_2}x_{2,j} \right|^2, \quad j = 1, 2, \dots, M_2, \quad (5)$$

where

$$y_{R_2}^{(*)} = y_{R_2} - \sqrt{P_s}h_{SR_2}\sqrt{\alpha_1}\hat{x}_1^{(*)}. \quad (6)$$

and

$$\hat{x}_1^{(*)} = \underset{k}{\operatorname{argmin}} \left| y_{R_2} - \sqrt{P_s\alpha_1}h_{SR_2}x_{1,k} \right|^2, \quad k = 1, 2, \dots, M_1, \quad (7)$$

¹The relay powers can be considered as shared among the relays with a PA β as being in [11]–[13]. Besides, the relays can harvest their transmit power from the RF signals in the first phase as in [16]. However, energy harvesting is not considered in this paper and it is beyond the scope of this paper.

²We could use joint maximum likelihood (JML) detector as proposed for the second phase rather than the SIC detector. However, the JML and SIC detectors have the same error performance in the downlink NOMA [17]. Besides, the JML costs a computational complexity as discussed in Section III. Therefore, the SIC detector is chosen.

2) *Decoding at the destination:* At the destination, both symbols (i.e., x_1 and x_2) should be detected. Indeed, it can be achieved by a SIC detector likewise at R_2 in the first phase. However, unlike the first phase, symbols are exposed to different channel fading coefficients in the second phase (uplink NOMA), and it is known that in the uplink NOMA, the SIC detector does not perform well so that an error floor occurs. Hence, the NOMA-DRN would have a poor error performance. On the other hand, the JML has a better performance in detecting signals for uplink NOMA. To this end, in the second phase, the destination implements a JML detector and it is given as

$$\begin{aligned} [\tilde{x}_1, \tilde{x}_2] = \underset{j,k}{\operatorname{argmin}} \left| y_D - \sqrt{P_{R_1}} h_{R_1 D} x_{1,k} - \sqrt{P_{R_2}} h_{R_2 D} x_{2,j} \right|^2, \\ j = 1, 2, \dots, M_2, \quad k = 1, 2, \dots, M_1, \end{aligned} \quad (8)$$

where \tilde{x}_1, \tilde{x}_2 are the detected symbols at the destination of x_1 and x_2 , respectively.

III. PERFORMANCE METRICS

A. Bit Error Rate (BER)

Since x_1 and x_2 are two consecutive symbols of the destination, the overall BER performance of the NOMA-DRN can be obtained by averaging BERs of two symbols. It is given by

$$P_{NOMA-DRN}(e) = \frac{P_1(e) + P_2(e)}{2} \quad (9)$$

where $P_1(e)$ and $P_2(e)$ are the e2e BER of the x_1 and x_2 symbols, respectively.

The e2e BERs of the symbols are defined as

$$\begin{aligned} P_i(e) &= \frac{1}{M_i} \sum P(x_i \rightarrow \tilde{x}_i) \quad i = 1, 2 \\ &= \frac{1}{M_i} \sum_j \sum_{m \neq j} P(x_{i,j} \rightarrow x_{i,m}) \end{aligned} \quad (10)$$

where $P(x_i \rightarrow \tilde{x}_i)$ denotes the pairwise error probability (PEP) when x_i is transmitted at the source and detected as \tilde{x}_i at the destination. Hence, it is derived by averaging all points in the constellation. Moreover, since the e2e communication consists of two phases and the relay has a DF protocol, the e2e PEP is turns out to be

$$\begin{aligned} P(x_i \rightarrow \tilde{x}_i) = \\ P(x_i \rightarrow \hat{x}_i) + P(\hat{x}_i \rightarrow \tilde{x}_i) - P(x_i \rightarrow \hat{x}_i) \cap P(\hat{x}_i \rightarrow \tilde{x}_i) \end{aligned} \quad (11)$$

where $P(x_i \rightarrow \hat{x}_i)$ and $P(\hat{x}_i \rightarrow \tilde{x}_i)$ are the PEPs in the first phase and second phase, respectively. Thus, intersection of them is subtracted to obtain the e2e PEP. Considering this, the e2e BERs of the symbols are given as

$$P_i(e) = 1 - \left(1 - P_i^{(S-R)}(e)\right) \left(1 - P_i^{(R-D)}(e)\right) \quad (12)$$

where $P_i^{(S-R)}(e)$ and $P_i^{(R-D)}(e)$ denote the BER of the first phase and the second phase, respectively. They are defined

as given in (10). However, since the transmission strategies differ in two phases (i.e., downlink and uplink NOMA), they are not the same. The $P_i^{(S-R)}(e)$ can be found in [18, eq.(4)] and [18, eq.(11)] over Nakagami-m fading channels. On the other hand, $P_i^{(R-D)}(e)$ of JML detector is obtained in [15, eq.(7)] and [15, eq.(10)] for only Rayleigh fading channels. By substituting these equations into (12) and then by substituting (12) into (9), the BER of the NOMA-DRN with the JML is obtained.

B. Diversity

The diversity order of the NOMA-DRN is given by

$$\nu = \lim_{SNR \rightarrow \infty} \frac{\log P_{NOMA-DRN}}{\log SNR} \quad (13)$$

Since the $P_{NOMA-DRN}$ is the average of $P_1(e)$ and $P_2(e)$, the diversity order of the NOMA-DRN is given by

$$\nu = \min\{\nu_1, \nu_2\} \quad (14)$$

where ν_1 and ν_2 are the diversity orders of the symbols x_1 and x_2 , respectively. Moreover, since a cooperative communication is included, the diversity order of the symbols is limited by the weakest link. Thus, it is given that

$$\nu_i = \min\{\nu_i^{(S-R)}, \nu_i^{(R-D)}\} \quad (15)$$

where $\nu_i^{(S-R)}$ and $\nu_i^{(R-D)}$ are given the diversity orders of the x_i symbols in the first phase (downlink NOMA) and in the second phase (uplink NOMA), respectively. The diversity order of x_i in the downlink NOMA is given as m_{SR_i} in [18]. On the other hand, the diversity order of the uplink NOMA with the JML is given for Rayleigh fading channels as the number of receiving antennas (i.e., 1 in this paper.) With the extension to the Nakagami-m fading channels, it can be said as the $m_{R_i D}$. However, this is only valid in the low-medium SNR region. With the increase of the SNR, the difference between the channel qualities/transmit powers becomes dominant on the diversity order rather than the shape parameters and the diversity order of the uplink NOMA in the high SNR region is limited by 1. To this end, by substituting these into (15) and then into (14), the diversity order of the NOMA-DRN with the JML in the low-medium SNR region is obtained as

$$\nu = \min\{m_{SR_1}, m_{SR_2}, m_{R_1 D}, m_{R_2 D}\}. \quad (16)$$

whereas it is limited by $\nu = 1$ in the high SNR region.

C. Complexity

In this section, we provide a comparison between the SIC based NOMA-DRN and the proposed NOMA-DRN with the JML in terms of the receiver complexity at the destination. The receivers complexities of the relays are not considered since they are the same in both the SIC based NOMA-DRN and the proposed NOMA-DRN with the JML. For the complexity compassion, we derive the number of the required complex operations. To obtain that, according to (5)-(7) (it is similar for the SIC detector at the destination), the SIC detector firstly generates M_1 candidates for the detection of

TABLE I
COMPLEXITY COMPARISONS BETWEEN SIC AND JML DETECTORS

M	SIC detector				JML detector			
	Adder	Multiplier	Comparator	Total	Adder	Multiplier	Comparator	Total
2	5	8	2	15	8	12	3	23
4	9	16	6	31	32	48	15	95
8	17	32	14	63	128	192	63	383
16	33	64	30	127	512	768	255	1535

the x_1 symbols, then it calculates the Euclidean distances and choose the minimum one by comparing. After detecting the x_1 symbols, it subtracts its regenerated form from the received signal. Finally, the above steps are repeated for the detection of x_2 symbols with M_2 candidates. Therefore, by considering $M_1 = M_2 = M$ (for notation simplicity), the required complex operations is given as

$$\delta_{SIC} = \underbrace{2M+1}_{\text{Adder}} + \underbrace{4M}_{\text{Multiplier}} + \underbrace{2(M-1)}_{\text{Comparator}} = 8M - 1 \quad (17)$$

On the other hand, in the JML detector as given in (8), the joint $M_1 \times M_2$ candidates are generated and the Euclidean distances are computed for each. Then, the minimum is obtained within these distances. To this end, the complexity of the JML detector is obtained as

$$\delta_{JML} = \underbrace{2M^2}_{\text{Adder}} + \underbrace{3M^2}_{\text{Multiplier}} + \underbrace{M^2-1}_{\text{Comparator}} = 6M^2 - 1. \quad (18)$$

In order to compare the complexities of both receivers, we present the total number of complex operations for different modulation sizes in Table I. As one can easily see that the complexity of the JML is negligible when M is relatively low. On the other hand, it increases exponentially with the increase of M. However, by considering the performance gain (as discussed in the next section), this complexity increase is affordable. Besides, because of this complexity, as we discussed in the Section 2, we implement SIC based detectors at the relay since both the SIC and JML detectors have the same error performance in downlink NOMA.

IV. NUMERICAL RESULTS

In this section, we present computer simulations to evaluate the BER performance of the proposed NOMA-DRN with the JML. Besides, we also provide comparisons with the conventional NOMA-DRN with the SIC detectors. For fair comparisons with [13], in the simulations, we consider a total transmit power for the relays (i.e., P_R) and it is shared among the relays as $P_{R_1} = \beta P_R$ and $P_{R_2} = (1 - \beta)P_R$. In simulations, $P_s = P_R$ is assumed. Firstly, we present BER simulations when $m_{SR_1} = m_{SR_2} = m_{R_1D} = m_{R_2D} = 1$ (Rayleigh fading) in Fig. 2 to compare the results with [13]. In Fig. 2, the shape parameters are $\Omega_{SR_1}^2 = 2$, $\Omega_{SR_2}^2 = 10$, $\Omega_{R_1D}^2 = 9$, $\Omega_{R_2D}^2 = 3$. The PA coefficients are assumed to be $\alpha = 0.9602$ and $\beta = 0.8011$ as the same with [13] and noted as the optimum values in [11]. The modulation orders are selected as BPSK for both symbols. In the simulations, we give results for the BERs of both symbols and for averaged

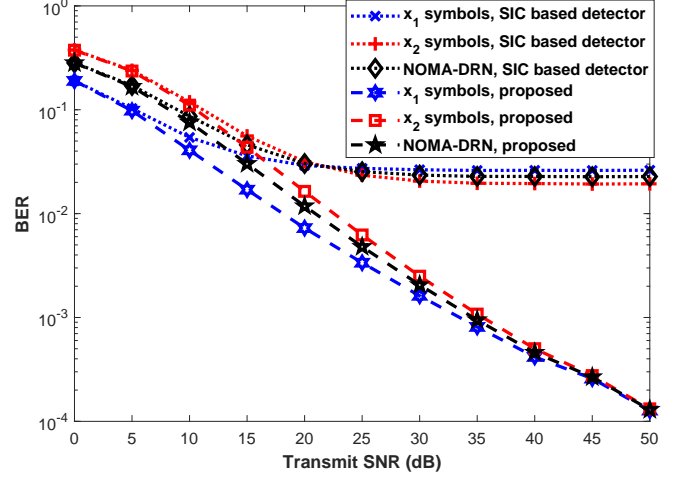


Fig. 2. BER Comparisons of the NOMA-DRN with SIC-based detector and the proposed JML detector over Rayleigh fading channels when $\Omega_{SR_1}^2 = 2$, $\Omega_{SR_2}^2 = 10$, $\Omega_{R_1D}^2 = 9$, $\Omega_{R_2D}^2 = 3$, $\alpha = 0.9602$ and $\beta = 0.8011$

NOMA-DRN. As seen in Fig. 2, with the proposed JML in the second phase, the error performance of the NOMA-DRN has been improved significantly and an error floor does not exist any more.

To reveal the effects of the shape parameters on the diversity order, we present simulation results over Nakagami-m fading channels for $m_{SR_1} = m_{SR_2} = m_{R_1D} = m_{R_2D} = 0.5$, $m_{SR_1} = m_{SR_2} = m_{R_1D} = m_{R_2D} = 2$ and $m_{SR_1} = m_{SR_2} = m_{R_1D} = m_{R_2D} = 3$ in Fig. 3. The spread parameters are the same with Fig. 2. As seen in Fig. 3, the diversity order of the NOMA-DRN with JML is equal to the shape parameters (i.e., 0.5, 2 and 3) for all scenarios in the low-medium SNR region. On the other hand, in the high SNR region it is limited by 1 when the shape parameter is greater than 1. Nevertheless, with the increase of shape parameters, a horizontal performance gain is achieved although the diversity order is not changed. For instance, the NOMA-DRN with shape parameters 3 has ~ 10 dB better performance than the scenario with the shape parameters of 2. Furthermore, regardless of the channel conditions, the proposed NOMA-DRN with JML outperforms the NOMA-DRN with the SIC detectors significantly. The proposed NOMA-DRN has no error floor and the performance gain over the SIC detector is up to $\sim 20 - 25$ dB in some scenarios.

TABLE II
SHAPE AND SPREAD PARAMETERS IN FIG. 4 AND FIG. 5

Scenario	m_{SR_1}	Ω_{SR_1}	m_{SR_2}	Ω_{SR_2}	m_{R_1D}	Ω_{R_1D}	m_{R_2D}	Ω_{R_2D}
I	3	1	3	10	1	10	1	1
II	3	5	3	10	1	10	1	5
III	1	1	1	10	3	10	3	1

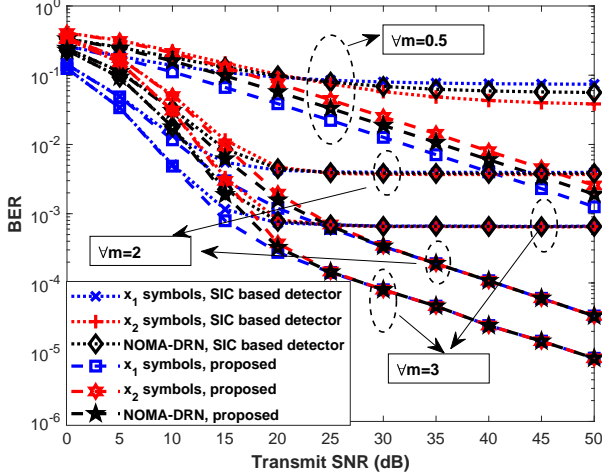


Fig. 3. BER Comparisons of the NOMA-DRN with SIC-based detector and the proposed JML detector over Nakagami- m fading channels with different shape parameters when all shape parameters are the same ($\forall m = 0.5, 2, 3$) $\Omega_{SR_1}^2 = 2$, $\Omega_{SR_2}^2 = 10$, $\Omega_{R_1D}^2 = 9$, $\Omega_{R_2D}^2 = 3$, $\alpha = 0.9602$ and $\beta = 0.8011$

Moreover, to show the effect of the minimum shape parameter and the spread parameters, in Fig. 4, we present the error performance of the NOMA-DRN with the JML for different scenarios. The parameters in each scenario are given in Table II. As seen in Fig. 4, all scenarios have the diversity order of the 1 since the minimum shape parameters between nodes is equal to 1. Nevertheless, according to the spread parameters, the error performance of the system changes. For instance, between Scenario I and II, the error performance of the x_1 symbols gets worse since the channel qualities difference between $R_1 - D$ and $R_2 - D$ becomes less so that the error performance of the second phase (uplink NOMA) is decreased. Hence, this decrease dominates the e2e performance of the x_1 symbols although the Ω_{SR_1} is increased. On the other, the second phase performance (uplink NOMA) of the x_2 symbols is increased with the increase of the Ω_{SR_1} . Thus, the overall performance of the NOMA-DRN in Scenario II is better than the Scenario I. Compared the Scenario I and III, although the both scenarios have the same diversity order, the Scenario III has better error performance. This explained as follows. In scenario III, with the increase of the shape parameters between the relays and the destination ($1 \rightarrow 3$), the error performance of the second phase (uplink NOMA) is improved and the second phase of the communication limits the error

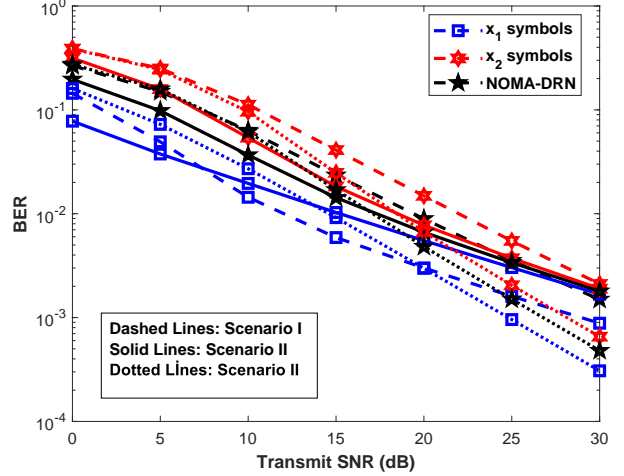


Fig. 4. BER of the NOMA-DRN with the proposed JML detector over Nakagami- m fading channels for the scenarios given in Table II

performance of the NOMA-DRN. Thus, this improvement provides a gain in overall performance of the NOMA-DRN. To validate above discussions, we provide the error performances of the both phases in Fig. 5. One can easily see that, although it is increased by the JML detector, the second phase (uplink NOMA) has worse performance than the first phase (downlink NOMA). Therefore, when the second phase performance is better, the NOMA-DRN has a good error performance.

V. CONCLUSION

In this paper, we propose a novel NOMA-DRN with the JML at the destination. We demonstrate the error performance of the proposed network and proved that the NOMA-DRN has not an error floor unlike the benchmark (NOMA-DRN with the SIC detector.) It outperforms remarkably the benchmark and a reliable communication can be accomplished with the increased spectral efficiency compared to the conventional CRS schemes. Furthermore, we also provide diversity analysis and the complexity analysis for the proposed network. We present that the proposed network can achieve full diversity order in the low-medium SNR region and the receiver complexity is affordable by considering the error performance gain. Moreover, the proposed model can save transmit energy up to $\sim 20 - 30dB$ compared to the benchmark. This is very promising for the energy-constrained networks such as IoT.

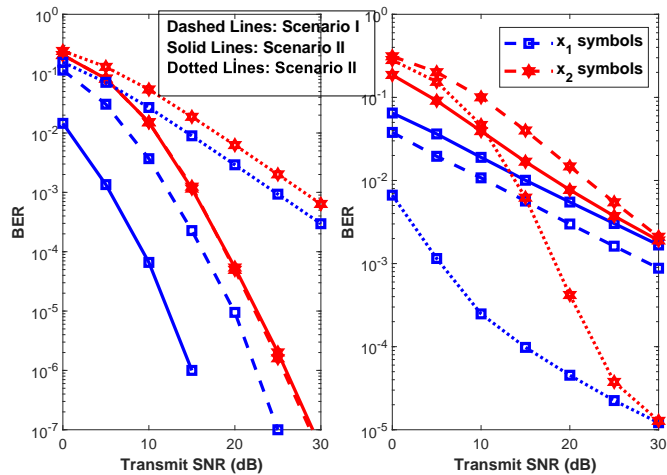


Fig. 5. BER of the both phases in the NOMA-DRN with the JML for the scenarios given in Table II a) First phase (downlink NOMA) b) Second phase (uplink NOMA)

REFERENCES

- [1] J. N. Laneman, D. N. C. Tse, and G. W. Wornell, "Cooperative diversity in wireless networks: Efficient protocols and outage behavior," *IEEE Trans. Inf. Theory*, vol. 50, no. 12, pp. 3062–3080, 2004.
- [2] J.-B. Kim and I.-H. Lee, "Capacity Analysis of Cooperative Relaying Systems Using Non-Orthogonal Multiple Access," *IEEE Commun. Lett.*, vol. 19, no. 11, pp. 1949–1952, 2015.
- [3] Y. Saito, Y. Kishiyama, A. Benjebbour, T. Nakamura, A. Li, and K. Higuchi, "Non-Orthogonal Multiple Access (NOMA) for Cellular Future Radio Access," in *2013 IEEE 77th Veh. Technol. Conf. (VTC Spring)*. IEEE, jun 2013, pp. 1–5.
- [4] R. Jiao, L. Dai, J. Zhang, R. Mackenzie, and M. Hao, "On the Performance of NOMA-Based Cooperative Relaying Systems Over Rician Fading Channels," *IEEE Trans. Veh. Technol.*, vol. 66, no. 12, pp. 11 409–11 413, 2017.
- [5] M. Xu, F. Ji, M. Wen, and W. Duan, "Novel Receiver Design for the Cooperative Relaying System with Non-Orthogonal Multiple Access," *IEEE Commun. Lett.*, vol. 20, no. 8, pp. 1679–1682, 2016.
- [6] Y. Zhang, Z. Yang, Y. Feng, and S. Yan, "Performance Analysis of Cooperative Relaying Systems with Power-Domain Non-Orthogonal Multiple Access," *IEEE Access*, vol. 6, pp. 39 839–39 848, 2018.
- [7] O. Abbasi, A. Ebrahimi, and N. Mokari, "NOMA inspired cooperative relaying system using an AF relay," *IEEE Wirel. Commun. Lett.*, vol. 8, no. 1, pp. 261–264, 2019.
- [8] M. F. Kader, M. B. Uddin, S. M. Islam, and S. Y. Shin, "Capacity and outage analysis of a dual-hop decode-and-forward relay-aided NOMA scheme," *Digit. Signal Process. A Rev. J.*, vol. 88, pp. 138–148, 2019.
- [9] F. Kara and H. Kaya, "Error performance of NOMA-based Cooperative Relaying Systems and Power Optimization for Minimum BER," *submitted.*, 2020.
- [10] J. B. Kim, M. S. Song, and I. H. Lee, "Achievable rate of best relay selection for non-orthogonal multiple access-based cooperative relaying systems," *2016 Int. Conf. Inf. Commun. Technol. Converg. ICTC 2016*, vol. 2, no. 3, pp. 960–962, 2016.
- [11] D. Wan, M. Wen, F. Ji, H. Yu, and F. Chen, "On the achievable sum-rate of NOMA-based diamond relay networks," *IEEE Trans. Veh. Technol.*, vol. 68, no. 2, pp. 1472–1486, 2019.
- [12] B. Huang, Y. Lee, and S. Sou, "Joint power allocation for noma-based diamond relay networks with and without cooperation," *IEEE Open Journal of the Communications Society*, vol. 1, pp. 428–443, 2020.
- [13] F. Kara and H. Kaya, "Error Probability Analysis of NOMA-Based Diamond Relaying Network," *IEEE Trans. Veh. Technol.*, vol. 69, no. 2, pp. 2280–2285, feb 2020.

- [14] F. Kara and H. Kaya, "BER performances of downlink and uplink NOMA in the presence of SIC errors over fading channels," *IET Commun.*, vol. 12, no. 15, pp. 1834–1844, 2018.
- [15] J. S. Yeom, H. S. Jang, K. S. Ko, and B. C. Jung, "BER Performance of Uplink NOMA with Joint Maximum-Likelihood Detector," *IEEE Trans. Veh. Technol.*, vol. 68, no. 10, pp. 10 295–10 300, 2019.
- [16] F. Kara, "Wireless Powered Cooperative Relaying Systems with Non-orthogonal Multiple Access," in *IEEE Int. Black Sea Conf. Commun. Netw.*, Odyssey, Ukraine, 2020.
- [17] A. Al-Dweik, T. Assaf, M. E. Moursi, H. Z. E. din, and M. Al-Jarrah, "Exact Bit Error-Rate Analysis of Two-User NOMA Using QAM with Arbitrary Modulation Orders," *tehrxiv*, 5 2020.
- [18] F. Kara and H. Kaya, "Derivation of the closed-form BER expressions for DL-NOMA over Nakagami-m fading channels," in *2018 26th Signal Process. Commun. Appl. Conf.* IEEE, may 2018, pp. 1–4.